DSC estimation of structural and textural parameters of SBA-15 silica using water probe

L. C. Cides da Silva · G. L. B. Araújo · N. R. Segismundo ·
E. F. Moscardini · L. P. Mercuri · I. C. Cosentino ·
M. C. A. Fantini · J. R. Matos

Abstract The aim of this study was to use DSC and X-ray diffraction measurements to determine the pore size and pore wall thickness of highly ordered SBA-15 materials. The DSC curves showed two endothermic events during the heating cycle. These events were due to the presence of water inside and outside of mesopores. The results of pore radius, wall thickness and pore volume measurements were in good agreement with the results obtained by nitrogen adsorption measurement, XRD and transmission electron microscopy.

L. C. Cides da Silva (✉) · J. R. Matos
Departamento de Química Fundamental, Instituto de Química, Universidade de São Paulo-USP, São Paulo 66083, Brazil
e-mail: luiscides@uol.com.br

G. L. B. Araújo
Departamento de Farmácia, Faculdade de Ciências Farmacêuticas, Universidade de São Paulo-USP, São Paulo 05508-000, Brazil

N. R. Segismundo · E. F. Moscardini · L. P. Mercuri
Departamento de Ciências Exates e da Terra, Universidade Federal de São Paulo-UNIFESP, Diadema, São Paulo 09972-270, Brazil

L. P. Mercuri
Departamento de Psicobiologia, Universidade Federal de São Paulo-UNIFESP, São Paulo 04032-020, São Paulo, Brazil

I. C. Cosentino
Centro de Ciência e Tecnologia de Materiais, Instituto de Pesquisas Energéticas e Nucleares-IPEN, São Paulo 05508-000, Brazil

M. C. A. Fantini
Departamento de Física Aplicada, Instituto de Física, Universidade de São Paulo-USP, São Paulo 053-970, Brazil

Introduction

In the 90's years researchers of the Mobil Oil Corporation developed a new family of ordered mesoporous sílica/aluminosilicate and designated this family of mesoporous materials as M41S [1, 2]. This discovery has, indeed, inspired scientists on a global scale to research creatively into the characterization, design, synthesis, modification, and application of these materials [3–5].

Since the pioneering research of Mobil scientists a whole new range of mesoporous materials have been synthesized. Recently, block copolymers have been used for synthesis of mesoporous materials, such as SBA-15 [6, 7] block copolymer template have been used for synthesis of mesoporous silica with large ordering and a variety of morphologies. Depending on the polymers used as template and synthesis process mesopores with different structures, however, with uniform pore diameters between 10 and 30 nm were formed. This silica is useful for application running from microelectronics to medical diagnosis, opening a wide variety of utilities beyond the traditional areas of materials for catalysis and absorbers [1–7].

Thermoporometry is a method of textural characterization which is based on the thermal analysis of the liquid-solid transformation of a pure capillary condensation inside the porous [8]. Recent articles report the low temperature constant rate thermodesorption as a tool to characterize porous solids [9, 10], melting and freezing behavior of water [11], benzene and cyclohexane [12] inside ordered mesoporous materials. Other techniques of thermal analysis were also used as tools to estimate the surface area and

porous volume in ordered mesoporous materials [13, 14]. Thermoanalytical techinques have also been used for sorption studies [15], characterization of mesoporous materials synthesized in different matrices [16], and determination of acid properties of semicristaline zeolitic mesoporous UL-ZSM-5 aluminesilicate [17].

From the synthesis of these materials with open cylindrical mesopores of uniform size it was possible to evaluate textural properties. The aim of this study was to use this technique to evaluate pore radius, wall thickness and porous volume of highly ordered mesoporous SBA-15 silica completed with the results of XRD studies, and comparing these results with those obtained by nitrogen adsorption and HRTEM.

Experimental

Materials

SBA-15 silica was synthesized as reported by Zhao et al. [6, 7], using Pluronic P123 triblock copolymer ($EO_{20}PO_{70}EO_{20}$) in acid media. DSC curves were recorded in a DSC-50 cell (Shimadzu) using open aluminum crucibles with about 20 mg of sample (SBA-15 silica + water, 1:3 in mass) under dynamic nitrogen atmosphere (100 mL min^{-1}) and cooling rate of 0.5 K min^{-1} from room temperature to 223 K and heating at a heating rate of 0.5 K min^{-1} to 298 K. DSC cell was cooled down using controlled liquid nitrogen flow by the aid of a TAC-50 (Shimadzu) cooling unit.

The small angle X-ray diffraction studies (XRD) were carried out using a rotating anode at 10 kW. The wavelength of the copper monochromatic X-ray beam was $\lambda = 1.5418$ Å. An image plate detector was utilized to record the scattering vector $q = (4\pi\sin\theta)/\lambda$, where θ denotes the half the scattering angle. The intensity was recorded for 1 h.

The pore width and pore wall thickness of SBA-15 were evaluated from the XRD unit cell parameter and primary mesopore volume using the geometrical method [18].

Adsorption isotherms were measured with Micromeritics ASAP 2010 volumetric adsorption analyzer using nitrogen of 99.998% purity. Measurements were performed in the range of relative pressure from 10^{-6} to 0.99 liquid nitrogen on the samples degassed for 2 h under reduced pressure at 473 K. The specific surface area was evaluated using BET method [19]. The total pore volume was estimated from the amount adsorbed at the relative pressure of 0.99. The pore size distribution (PSD) was calculated using BJH algorithm [20], with the relation between the capillary condensation pressure and the pore diameter established by Kruk et al. [21].

For TEM observations, the samples were studied using a JEM-3010 (Cs) 0.6 mm, resolution 0.17 nm) at 300 kV. High resolution transmission electron microscopy (HRTEM) images were recorded with a slow scan CCD (Gatan 794). The SBA-15 sample was dispersed in isopropyl alcohol and put on a holey carbon film on a Cu grid.

Results and discussion

Figure 1 shows the diffractogram for the SBA-15 silica sample. The diffraction peaks were indexed for (100), (110), (200), (210) and (300) reflections based on a hexagonal structure, space group p6 mm [6, 7]. The interplanar spacing (d_{hkl}) and the lattice parameter (a) were calculated for the (100), (110), (200) and (210) reflections. Figure 2a shows that Nitrogen adsorption isotherm for SBA-15 sample is similar to those ones reported by Zhao et al. [6, 7] and, Kruk and Jaroniec [22]. The isotherm of SBA-15 sample has shown hysteresis loop with sharp adsorption and desorption branch. The sharpness of the branched adsorption is an indicative of a narrow porous size distribution (PSD) shown in Fig. 2b. The branched adsorption was located at relative pressures in the 0.64–0.8 range, a high relative pressure, similarly to good-quality mesoporous materials [21, 22]. The BET specific surface area of the SBA-15 sample was 610 m^2 g^{-1} with pore size of 7.4 nm to the SBA-15 sample, these parameters were similar to the mesopore size for materials with honeycomb structures in good agreement with those reported by Zhao et al. [6, 7].

The uniform channels characteristics of the SBA-15 silica obtained was confirmed by the HRTEM image as shown in Fig. 3a. The pore size and the wall thickness average obtained were 6.7 and 6.1 nm, respectively, whose
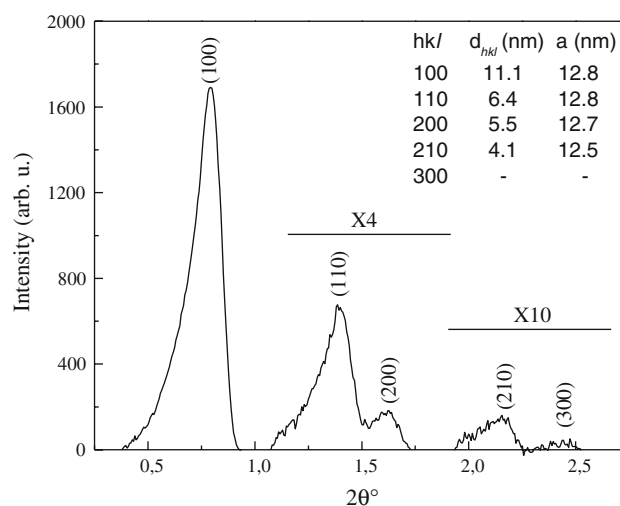
hkl	d_{hkl} (nm)	a (nm)
100	11.1	12.8
110	6.4	12.8
200	5.5	12.7
210	4.1	12.5
300	-	-

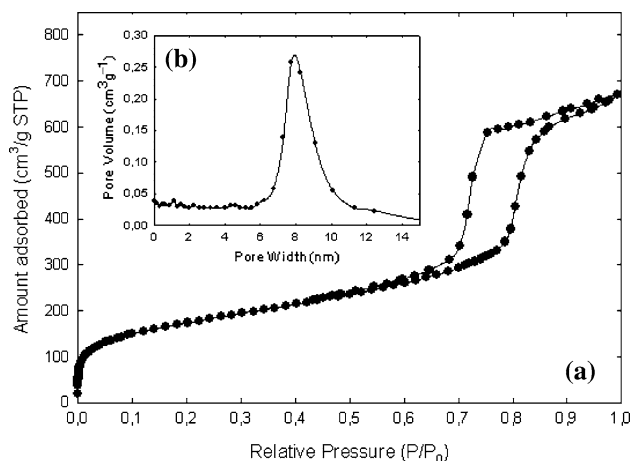Fig. 1 Small angle X-ray diffraction data for the SBA-15 silica sample

Fig. 2 a Nitrogen adsorption isotherm for the SBA-15 silica sample. **b** Pore size distribuition (PSD) for the SBA-15 silica sample
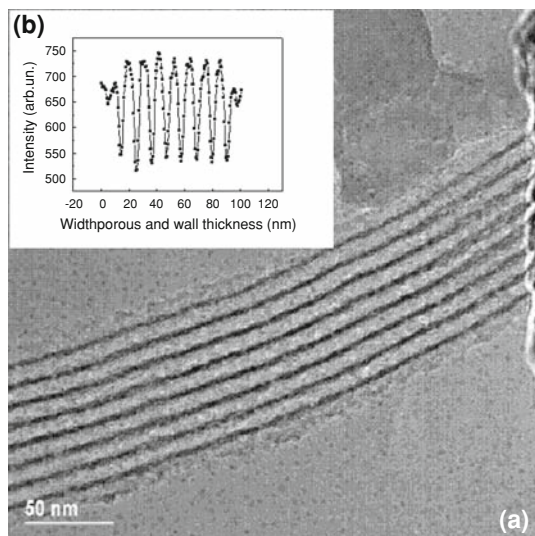

Fig. 3 a The HRTEM image of the cylindrical mesoporous of the sample of SBA-15 silica. **b** Distribution graph of porous width and wall thickness of the sample of SBA-15 silica

results were obtained by Fourier Transformed without image corrections (Fig. 3b). The DSC curve of water in SBA-15 sample exhibited two peaks upon heating. This event showed a sharp exothermic peak that corresponds to water melting inside mesopores at 260.03 K.

The second endothermic peak is observed at 271.88 K, regarding to the melting of water outside of the mesopores.

The first peak that corresponds to the melting point of water inside of mesopores (Fig. 4a) was used in Eq. 1 of Laundry [9] and Ishikiriyama et al. [23] to calculate the pore radius of the SBA-15 sample.

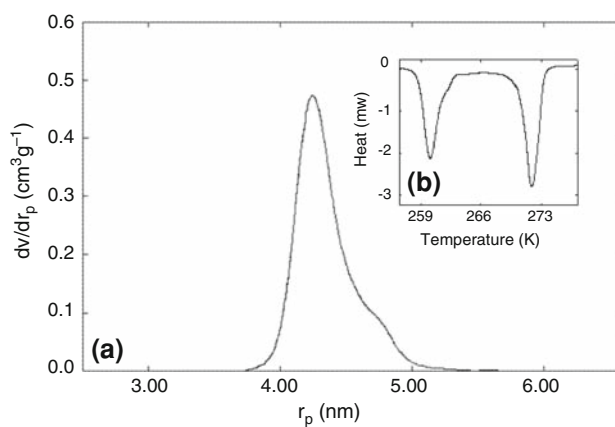$$R_p = \frac{-33.3}{\Delta T} - 0.32 + \delta m \tag{1}$$

Fig. 4 a Pore size distribution for porous size distribution of SBA-15 sample. **b** DSC curve for water in SBA-15 sample, showing two endothermic peaks, the first peak regarding water melting inside the mesoporous and the second peak regarding melting water outside the one

where, $\Delta T = (T_0 - T)$ is the decrease of melting temperature of water in mesopores and $\delta m = 1.12$ nm is the presence a thin film of non-freezable liquid adjacent to pore wall.

Total pore volume V_p (e.g., cm^3 g^{-1}) is another important parameter for characterizing porous materials [9]. A simple calculation of V_p can be made from a single thermoporometry heating experiment using the Eq. 2:

$$V_p = \frac{\Delta H_{\text{porous}} m_{\text{liq 1}}}{\Delta H_{\text{Total}} \ m_{\text{sol}} \rho_{\text{liq}}} \tag{2}$$

where liquid mass (m_{liq}), water density (ρ_{liq}), porous solid mass (m_{sol}), pore melt area (ΔH_{porous}) and excess melt peak areas (ΔH_{Total}) are parameters obtained from the DSC melt endotherms and their ratio is related to the fraction of liquid contained in the pores.

Equation 2 assumes a temperature-independent heat ΔH_{fusion} and liquid density, as well as a sufficient separation of the pore and excess melt peaks to independently integrate their areas. It is also assumed that all of the liquid has frozen during the initial quench cooling step and melts during heating, i.e., the contribution of the thin liquid layer adjacent to pore walls and other non-frozen liquid is negligible. Figure 4b shows a porous size distribution with a mean radius of 4.25 nm. Applying a heating rate to a melting sample an turning a nearly known mass of water gives a measure of the amount of pore liquid undergoing phase transition.

Table 1 shows comparative results between pore size and wall thickness average, with were obtained by analysis of nitrogen adsorption isotherm, transmission electronic microscopy and thermoporometry. The values of these parameters clearly show that data obtained by thermoporometry showed estimated values near to ones those obtained by conventional methods.

Table 1 Comparative results of the pore diameters and thickness of pore wall of the SBA-15 silica sample, obtained by thermoporometry associated with XDR; Nitrogen isotherm adsorption associated with XDR and TEM

SBA-15 sample	R_p/nm	W_p/nm	$d_{(100)}$/nm	a/nm	b_d/nm	V_p/cm^{3}g^{-1}
Thermoporometry	4.25	8.50	11.1	12.8	4.34	1.12
N_2 isotherm adsorption	5.85	11.7	11.1	12.8	1.10	0.92
TEM	*3.35	*6.7	11.1	12.8	*6.1	–

R_p = pore radius; W_p = pore width; $d_{(100)}$ = SAXRD interplanar spacing in the 100 direction; a = lattice parameter b_d = wall thickness

*Data obtained directly of the HRTEM image without correction

Conclusions

The water melting temperature determined by DSC inside and outside the pores allowed us to evaluate the radii of mesopores and wall thickness of SBA-15 sample. The current study demonstrates that DSC studies are important for characterization of ordered mesoporous materials and to evaluate their textural and structural quality properties. It is possible to estimate the porous radius and volume, wall thickness and surface area, associating DSC, XRD and TEM techniques. DSC gives preliminary information on the material properties that can be useful to decide if they are worth to perform further characterization by nitrogen adsorption isotherm and TEM, which are more accurate techniques, but require longer analysis time and imply in much more expensive measurements.

References

1. Kresge CT, Leonowics ME, Roth WJ, Vartuli JC, Beck JS. Ordered mesoporous molecular sieves synthesized by a liquid-crystal template mechanism. Nature. 1992;359:710–2.
2. Beck JS, Chu CT, Johnson ID, Kresge CT, Leonowicz ME, Roth WJ, Vartuli JC. US Patent 5,108,725 to Móbil Corporation; 1992.
3. Corma A, Kumar D. In: Catlow R, Cheethan A, editors. New trends in materials chemistry, NATO ASI Series, vol 498. Dordrecht: Kluwer Academic Publishers; 1997. p. 403.
4. Sayari A, Liu P. Non-silica periodic mesostructured materials: recent progress. Microporous Mater. 1997;12:149–77.
5. Anotelli DM, Ying JY. Curr Opin Colloid Interface Sci. 1996;1:523.
6. Zhao DY, Feng JL, Huo QS, Melosh N, Fredrickson GH, Chmelka BF, et al. Science. 1998;279:548.
7. Zhao DY, Huo QS, Feng JL, Chmelka BF, Stucky GD. Nonionic triblock and star diblock copolymer and oligomeric surfactant syntheses of highly ordered, hydrothermally stable, mesoporous silica structures. J Am Chem Soc. 1998;120:6024–36.
8. Quinson JF, Brun M. Charact Porous Solids. 1988;39:548.
9. Laundry MR. Thermochim Acta. 2005;433:433.
10. Chevrot V, Llewellyn PL, Roquerol F, Godlewski J, Roquerol J. Low temperature constant rate thermodesorption as a tool to characterise porous solids. Thermochim Acta. 2000;360:77–83.
11. Schreiber AF, Ketelsen I, Findenegg GH. Melting and freezing of water in ordered mesoporous silica materials. Phys Chem Chem Phys. 2001;3:1185–95.
12. Dosseh G, Xia Y, Alba-Simionesco C. Cyclohexane and benzene confined in MCM-41 and SBA-15: confinement effects on freezing and melting. J Phys Chem B. 2003;107:6445–53.
13. Mercuri LP, Matos JR, Jaroniec M. Thermogravimetric estimation of adsorption properties of europium-incorporated MCM-41 materials. Thermochim Acta. 2002;383:79–85.
14. Mercuri LP, Matos JR, Jaroniec M. Improved thermogravimetric determination of the specific surface area for cerium-incorporated MCM-41 materials. J Alloys Compd. 2002;344:190–4.
15. Goworek J, Kierys A, Iwan M, Stefaniak W. Sorption on as-synthesized MCM-41. J Therm Anal Calorim. 2007;87:165–9.
16. Berezovska IS, Yanishpolskii VV, Tertykh VA. Synthesis of mesoporous silicas inside large pores of inorganic matrix. J Therm Anal Calorim. 2008;94:649–53.
17. Ungureanu A, Thang HV, On DT, Dumitriu E, Kaliaguine S. Acid properties of semicrystalline zeolitic mesoporous UL-ZSM-5 materials. J Therm Anal Calorim. 2007;87:417–22.
18. Kruk M, Jaroniec M, Sakamoto Y, Terasaki O, Ryoo R, Ko CH. Determination of pore size and pore wall structure of MCM-41 by using nitrogen adsorption, transmission electron microscopy, and X-ray diffraction. J Phys Chem B. 2000;104:292–301.
19. Brunauer S, Emmet PH, Teller E. Adsorption of gases in multi-molecular layers. J Am Chem Soc. 1938;60:309–19.
20. Barret EP, Joyner LG, Halenda PH. The determination of pore volume and area distributions in porous substances. I. Computations from nitrogen isotherms. J Am Chem Soc. 1951;73:373–80.
21. Kruk M, Jaroniec M, Sayari A. Application of large pore MCM-41 molecular sieves to improve pore size analysis using nitrogen adsorption measurements. Langmuir. 1997;13:6267–73.
22. Kruk M, Jaroniec M. Characterization of the porous structure of SBA-15. Chem Mater. 2000;12:1961–8.
23. Ishikiriyama K, Todoki M, Motomura K. Pore size distribution (PSD) measurements of silica gels by means of differential scanning calorimetry: I. Optimization for determination of PSD. J Colloid Interface Sci. 1995;171:92–102.